Title: Power System Dynamic Paper Discussion

Subject: On the effect of AVR gain on bifurcations of sub synchronous resonance

Mohammad S.Widyan

Electrical Engineering Department , The Hashemite University,13115 Zarqa , Jordan

Elsevier journal , Electrical Power and Energy Systems,2010

First Name: Mehrdad

Last Name: Keshavarz

Student Number: 9131054

Electrical and Computer Engineering Department, shiraz University , Shiraz , Iran

Introduction:

Series capacitor compensation of AC transmission lines is an effective way of increasing load carrying capability and enhancing transient stability beside the capability of VAR and voltage controlling.

Until about 1971, it was generally believed that up to 70% series compensation could be used in any transmission line with little or no concern. however, when in 1970, and again in 1971, a 750MW cross compound Mohave turbine-generator in southern Nevada experienced shaft damage it is learn that series capacitors can create an adverse interaction between the series compensated electrical system and the spring mass mechanical system of the turbine-generators. this effect is called **subsynchronous resonance** (SSR) since it is the result of a resonant condition, which has a natural frequency below the fundamental frequency of power system.

SSR can be studied through many methods, eigenvalue analysis frequency scanning technique, frequency response analysis and time domain analysis.

In the last few years power system dynamics have been studied from nonlinear dynamics point of view using bifurcation theory. the most commonly encountered bifurcation is the dynamic bifurcation "**Hopf bifurcation**" in which a pair of complex conjugate eigenvalues of the linearized model around an operating point transversally crosses the imaginary axis of the complex plane resulting in born of a limit cycle.

In this paper the objective is to investigate the effect of AVR gain on bifurcation of subsynchronous resonance. The IEEE second benchmark model of SSR is chosen for the numerical investigation.

Bifurcation theory

Bifurcation is a qualitative and /or quantitative change in the behavior of a nonlinear system when one or more of its parameters change. For example, the stability of an equilibrium solution change from locally asymptotically stable to unstable at certain values of the system parameters. These changes are called bifurcations and the parameter values at which the changes occur are called bifurcation values.

Consider the following nonlinear dynamical autonomous system:

$$\frac{dx}{dt} = F(x; \mu)$$

Where μ is the bifurcation parameter. The equilibrium solutions are obtained by dropping out all the time derivative terms and solving the resulted nonlinear set of algebraic equations:

$F(x, \mu) = 0$

Let the solution for $\mu=\mu_0$ be x_0. To determine the stability of this equilibrium solution, a small disturbance y is superimposed on it i.e.

$x(t)=x_0+y(t)$

Then we have this equation:

$$\frac{dy}{dt} = F(x_0 + y; \mu_0)$$

Expanding equation above in a Taylor series about x_0 and retaining only linear terms in the disturbance leads to

$$\frac{dy}{dt} = F(x_0;\mu_0) + D_x F(x_0;\mu_0)y + O(|y|^2)$$

Or $\frac{dy}{dt} \approx D_x F(x_0;\mu_0)y = Ay$

Where A is the matrix of the first partial derivatives at the operating point.it is called the Jacobean matrix. The eigenvalues of this constant matrix provides information about the local stability of the equilibrium solution x_0.It is said local because a small disturbance and linearizing the vector field is considered. If all of the eigenvalues of A have negative real parts, then all of the components of disturbance y decay in time, and x approaches the equilibrium x_0 as $t\rightarrow\infty$. Therefore the equilibrium solution x_0 is asymptotically stable.

A Hopf bifurcation of an equilibrium solution occurs if the following conditions are satisfied:

1-$F(x_0, \mu_0)=0$.

2-The matrix A has a pair of purely imaginary eigenvalues $\pm j\omega_h$ while the other eigenvalues have nonzero real parts at (x_0, μ_0).

3-For $\mu\approx\mu_0$ let the analytical continuation of the pair imaginary eigenvalues be $\lambda\pm j\omega$. then $(\frac{d\lambda}{d\mu})\neq 0$ at $\mu= \mu_0$.This condition implies a transversal or nonzero speed crossing of the imaginary axis and hence is called the transversality condition.

It is shown in some papers that these conditions are satisfied in the IEEE second benchmark model of SSR.

System description and mathematical model

The considered power system is shown in fig bellow, the first system of the IEEE second benchmark model of SSR, it is a SMIB (singe machine infinite bus) power system whit two transmission lines, on of them is compensated by a series capacitor.

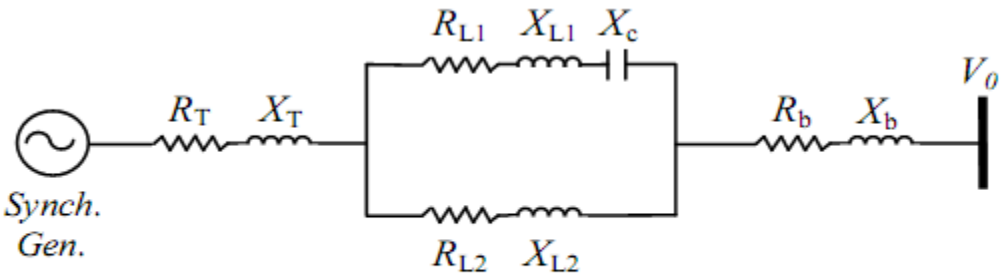

Fig. 1. First system of the IEEE second benchmark model

The single shaft turbine generator mechanical system consist of a high-pressure (HP) turbine, a low pressure turbine (LP), a generator and exciter as shown in Fig2.K,D and M parameters represent the spring coefficient, the damping coefficient and inertia constant of the corresponding shaft section, respectively. The system parameters are given in Appendix.

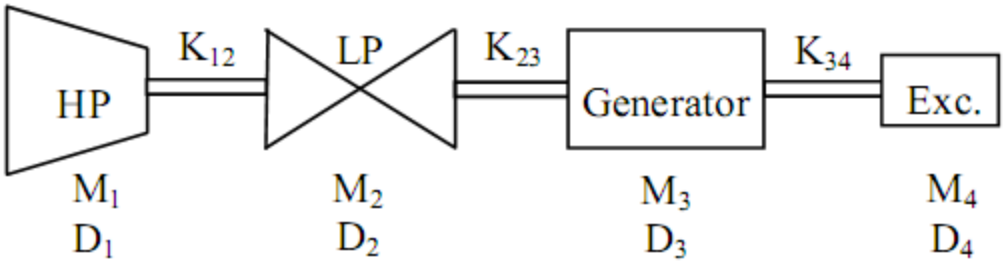

Fig. 2. Schematic diagram of the mechanical system consisting of a high-pressure (HP) turbine, a low-pressure turbine (LP), a generator and an exciter

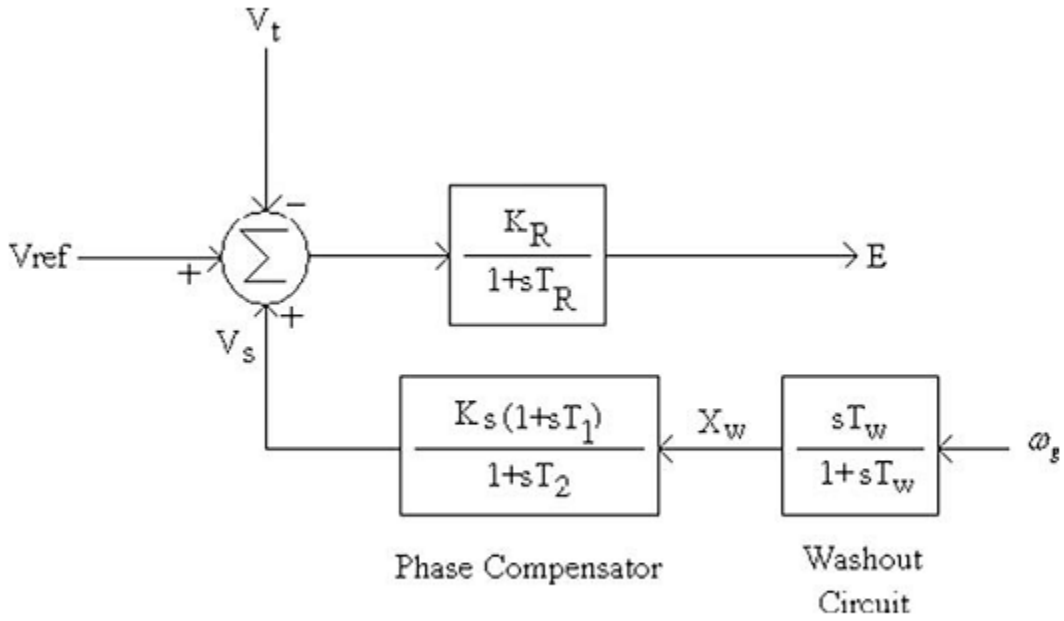

Fig. 3. Block diagram of the AVR and PSS.

The mathematical model of the system can be written as:

Synchronous generator

$$x_{ffd}\frac{di_{fd}}{dt} - x_{afd}\frac{di_d}{dt} + x_{fkd}\frac{di_{kd}}{dt} = \omega_0\frac{r_{fd}}{x_{afd}}E - \omega_0 r_{fd} i_{fd} \qquad (1)$$

$$x_{afd}\frac{di_{fd}}{dt} - (x_d + x_T + kx_{L1} + x_b)\frac{di_d}{dt} + x_{akd}\frac{di_{kd}}{dt} = \omega_0 V0\sin(\delta_g) + \omega_0(R_b + R_T + kR_{L1} + ra)i_d - \omega_0(x_T + x_b + kx_{L1} + \omega_g x_q)i_q + \omega_0\omega_g x_{akq} i_{kq} + \omega_0 v_{cd} \quad (2)$$

Where $k = \frac{\sqrt{{R_{L2}}^2 + {x_{L2}}^2}}{\sqrt{(R_{L1}+R_{L2})^2 + (x_{L1}+x_{L2}-\mu x_{L1})^2}}$ and $\mu = \frac{x_c}{x_{L1}}$; the compensation factor.

$$x_{fkd}\frac{di_{fd}}{dt} - x_{akd}\frac{di_d}{dt} + x_{kkd}\frac{di_{kd}}{dt} = -\omega_0 r_{kd} i_{kd} \quad (3)$$

$$-(x_q + x_T + kx_{L1} + x_b)\frac{di_q}{dt} + x_{akq}\frac{di_{kq}}{dt} = \omega_0 V0\cos(\delta_g) - \omega_0\omega_g x_{afd} i_{fd} + \omega_0(x_T + x_b + kx_{L1} + \omega_g x_q)i_d - \omega_0\omega_g x_{akd} i_{kd} + \omega_0(R_b + R_T + kR_{L1} + ra)i_q + \omega_0 v_{cq} \quad (4)$$

$$-x_{akq}\frac{di_q}{dt} + x_{kkq}\frac{di_{kq}}{dt} = -\omega_0 r_{kq} i_{kq} \quad (5)$$

Transmission line

$$\frac{dv_{cd}}{dt} = \omega_0 k\mu x_{L1} i_d + \omega_0 v_{cq} \quad (6)$$

$$\frac{dv_{cq}}{dt} = \omega_0 k\mu x_{L1} i_q - \omega_0 v_{cd} \quad (7)$$

Mechanical system

$$\frac{d\delta_1}{dt} = \omega_0\omega_1 - \omega_0 \quad (8)$$

$$M_1\frac{d\omega_1}{dt} = D_1 - D_1\omega_1 - k_{1g}\delta_1 + k_{1g}\delta_g \quad (9)$$

$$\frac{d\delta_g}{dt} = \omega_0\omega_g - \omega_0 \quad (10)$$

$$M_g \frac{d\omega_g}{dt} = T_m + D_g - x_{afd} i_q i_{fd} + x_d i_q i_d - x_{akd} i_{kd} i_q - x_q i_q i_d + x_{akq} i_{kq} i_d - D_g \omega_g + k_{1g}\delta_1 - k_{1g}\delta_g - k_{g2}\delta_g + k_{g2}\delta_2 \quad (11)$$

$$\frac{d\delta_2}{dt} = \omega_0 \omega_2 - \omega_0 \quad (12)$$

$$M_2 \frac{d\omega_2}{dt} = D_2 - D_2 \omega_2 + k_{g2}\delta_g - k_{g2}\delta_2 - k_{23}\delta_2 + k_{23}\delta_3 \quad (13)$$

$$\frac{d\delta_3}{dt} = \omega_0 \omega_3 - \omega_0 \quad (14)$$

$$M_3 \frac{d\omega_3}{dt} = D_3 - D_3 \omega_3 + k_{23}\delta_2 - k_{23}\delta_3 \quad (15)$$

AVR and PSS

$$T_w \frac{dx_w}{dt} - T_w \frac{d\omega_g}{dt} = -x_w \quad (16)$$

$$T_2 \frac{dV_s}{dt} - T_1 k_s \frac{dx_w}{dt} = k_s x_w - V_s \quad (17)$$

$$T_R \frac{dE}{dt} = k_R V_{ref} + k_R V_s - k_R V_t - E \quad (18)$$

Where $V_t = \sqrt{{V_d}^2 + {V_q}^2}$ neglecting stator transient yields:

$$V_t = \sqrt{(-r_a i_d + x_q i_q)^2 + (-r_a i_q - x_d i_d + x_{afd} i_{fd})^2}$$

Numerical simulations

In this section you can see the result of bifurcation analysis whit some time domain simulations. The bifurcation parameter is the compensation factor μ. Although whit increasing μ the power transfer capability increase but the operating point may not keep its stability at some compensation factors.

The variation of imaginary and real parts of the prime interest eigenvalues of the linearized model around the operating point whit k_R =100 is shown in fig3 and fig4 respectively. **You can see all the results in pair of this paper and that of mine. (the first one is of this paper and the second one is of mine).**

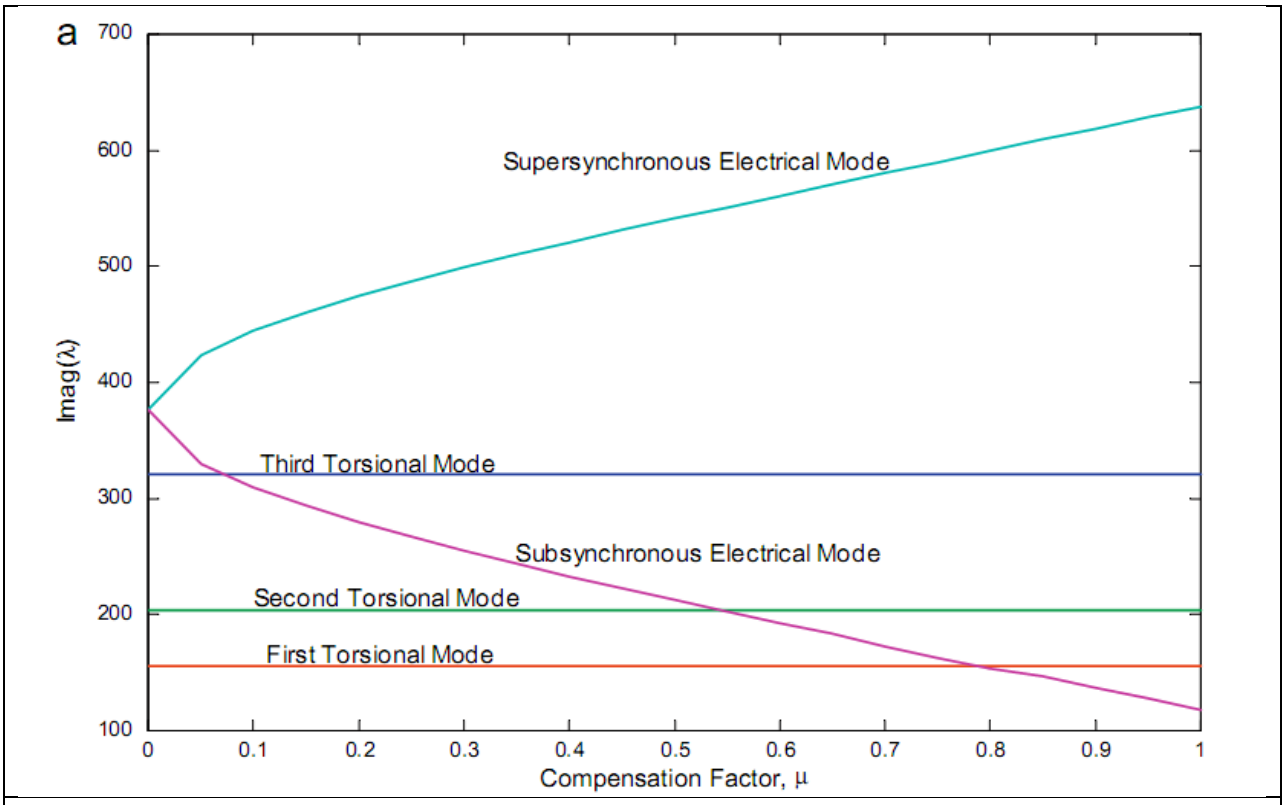

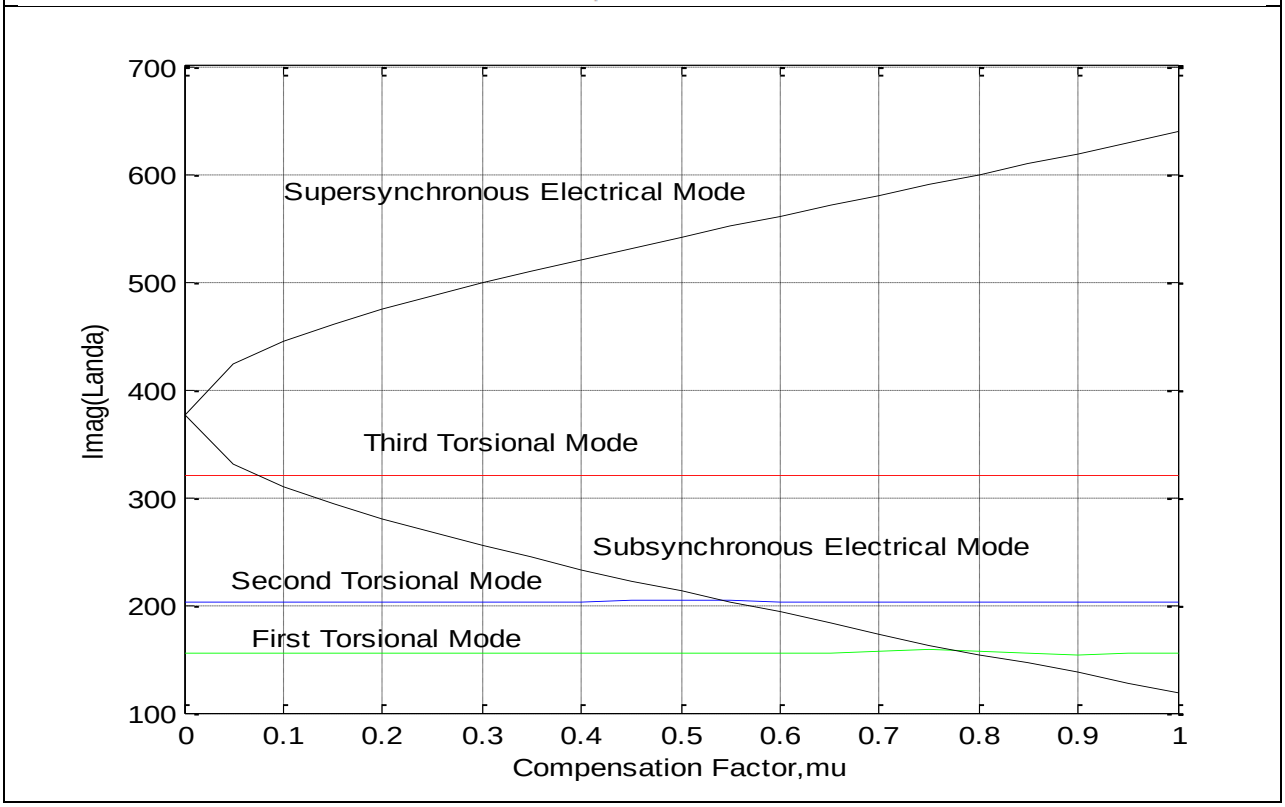

Fig3. Variation of imaginary parts of eigenvalues of the linearized model around the operating point as a function of μ whit k_R=100 ; the first one is of this paper and the second one is of mine.

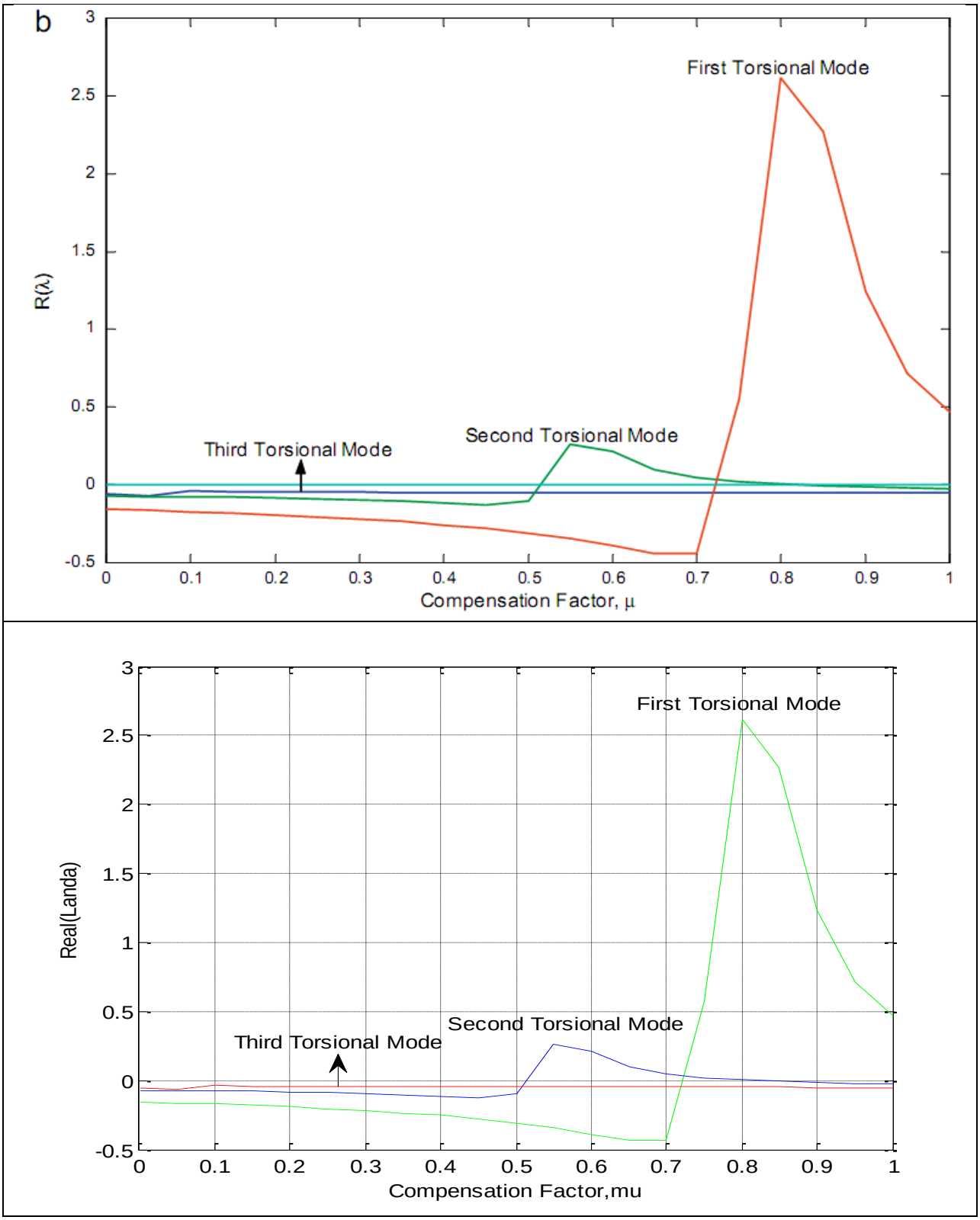

Fig4. Variation of real parts of eigenvalues of the linearized model around the operating point as a function of μ whit k_R=100 ; the first one is of this paper and the second one is of mine.

As shown in figs 3 and 4 as the compensation factor increases, the supersynchronous electrical mode increases while that of the subsynchronous decreases and intersects successively with the third, second and first torsional mechanical modes at $\mu \approx 0.0723$, 0.5455 and 0.7922, respectively. But the **Hopf bifurcation** point is at $\mu \approx 0.5210$, since the second interaction was able or strong enough to transversally move the corresponding real parts of eigenvalues from left-to the right-half of complex plane. The equilibrium stability regions are shown in the bifurcation diagram of fig .5 in δ_g-μ plane. The power system has a stable operating point in the region $0<\mu<0.5210$, unstable operating point in the region $0.5210<\mu<1$ and a Hopf bifurcation point at $\mu=H\approx 0.5210$.

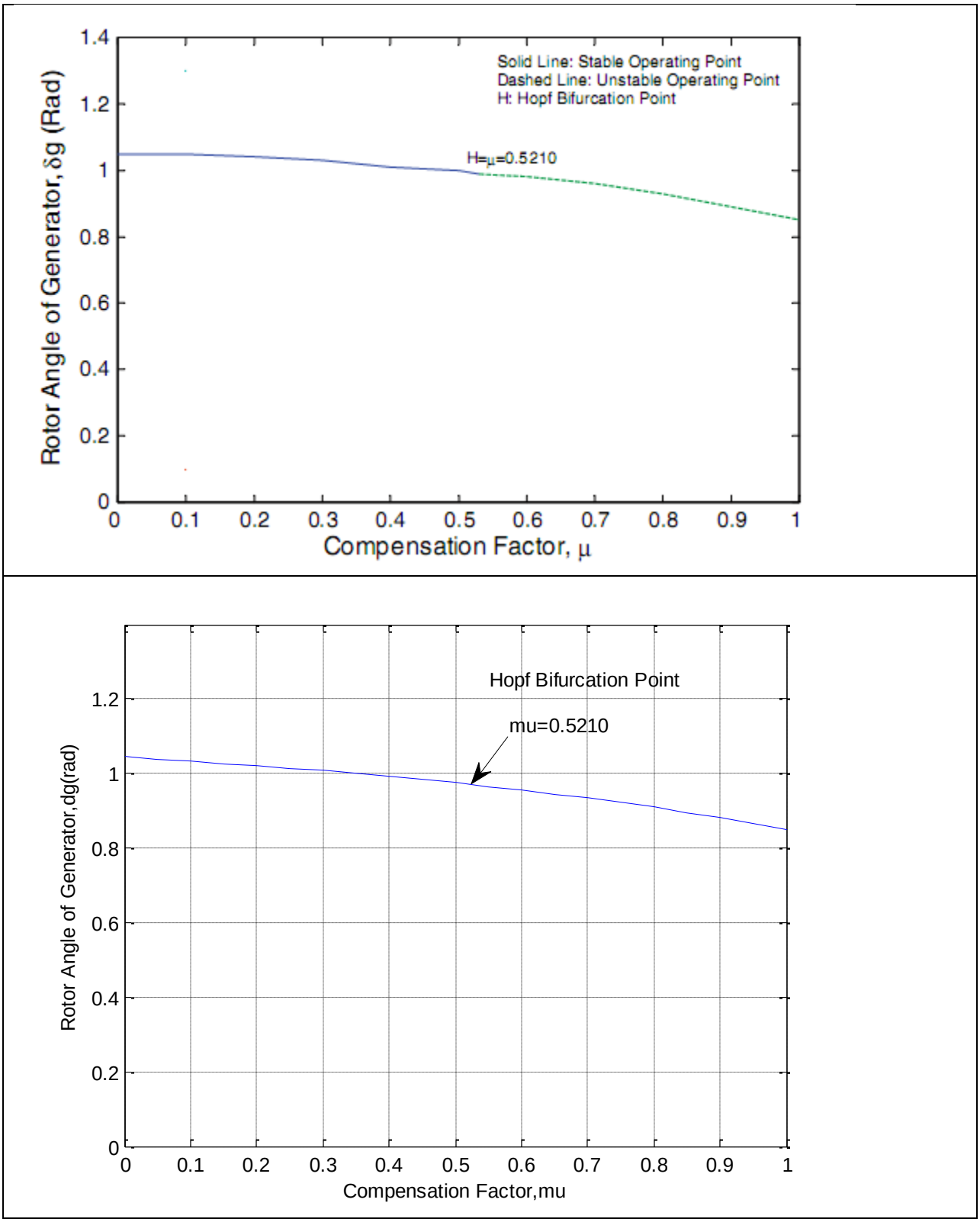

Fig5. Bifurcation diagram with k_R=100, rotor angle of generator δ_g as a function of the compensation factor μ; the first one is of this paper and the second one is of mine.

Now we reached a point at which we should determine the type of the dynamic bifurcation.

As before was said At Hopf bifurcation point ($\mu=H$) a limit cycle is born, this limit cycle is stable if the Hopf bifurcation is supercritical and unstable in case of subcritical Hopf bifurcation. The type of the Hopf bifurcation can be determined by numerical method based on the response of the perturbed system. If the system loses the stability at $\mu=H-\varepsilon$ then, the bifurcation is subcritical, while in case of supercritical bifurcation, the system will route to a periodic solution giving rise to oscillations at $\mu=H+\varepsilon$.Fig.6 shows the response of the system(rotor angle of generator δ_g) after a 9% initial disturbance on the speed of the generator at $\mu=0.515$,(slightly before the Hopf bifurcation point $\mu=H\approx0.5210$).clearly the system routes to unpredictable solution which indicates that the Hopf bifurcation is of subcritical type.

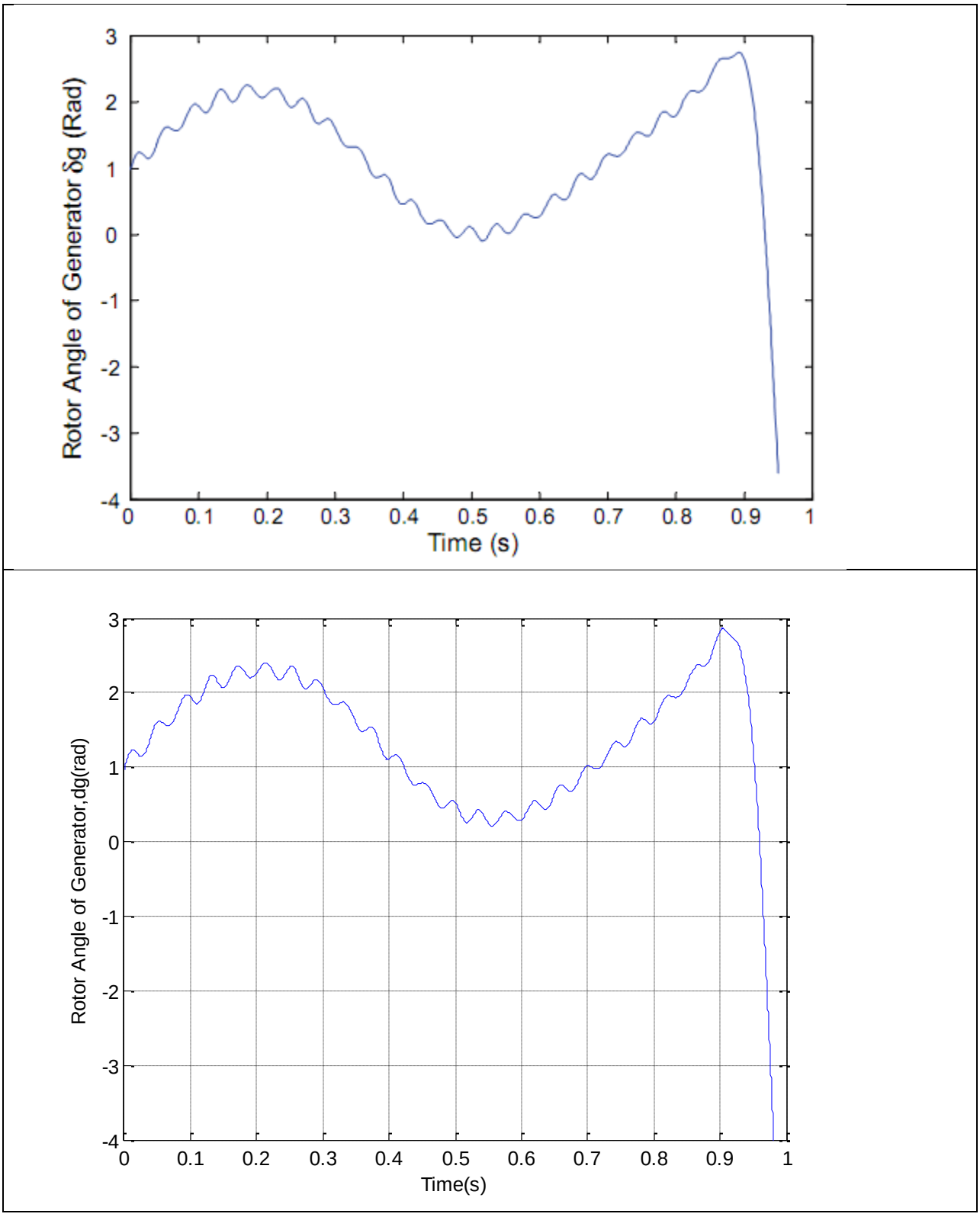

Fig6. Rotor angle of generator δ_g after 9% initial disturbance on the speed of the generator at μ=0.515(slightly before the Hopf bifurcation point); the first one is of this paper and the second one is of mine.

The operating point bifurcations of the system with k_R equals 1000 is repeated in fig7.The Hopf bifurcation occurred at $\mu=H\approx0.6363$ (it was at $\mu=0.5210$ in the previous case when $k_R=100$).

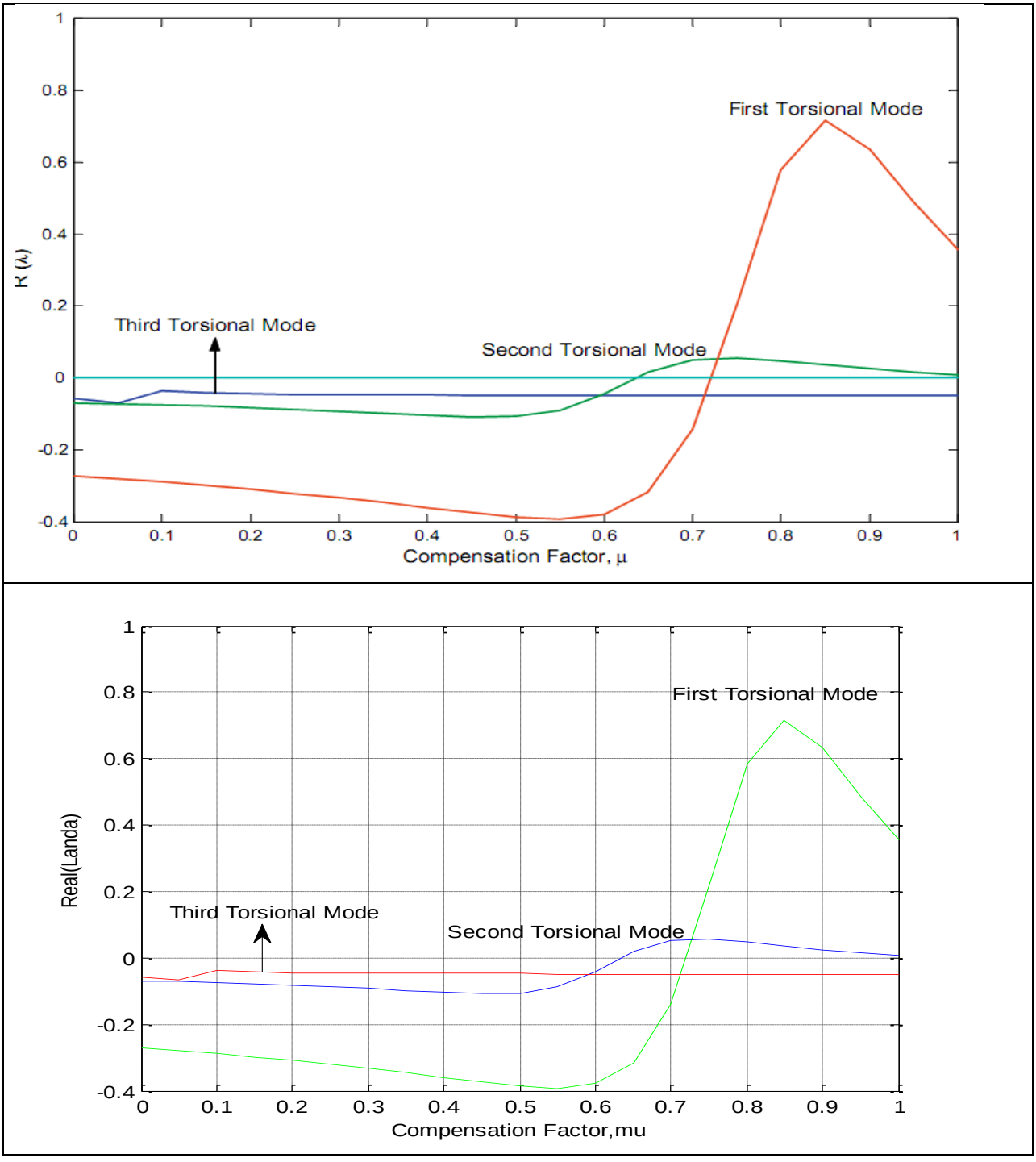

Fig7. Variation of real parts of eigenvalues of the linearized model around the operating point as a function of μ whit $k_R=1000$; the first one is of this paper and the second one is of mine.

The bifurcation diagram for this case is shown in fig8.The operating point is stable in the region $0<\mu<0.6363$, unstable in the region $0.6363<\mu<1$ and a Hopf bifurcation point at $\mu=H\approx0.6363$.

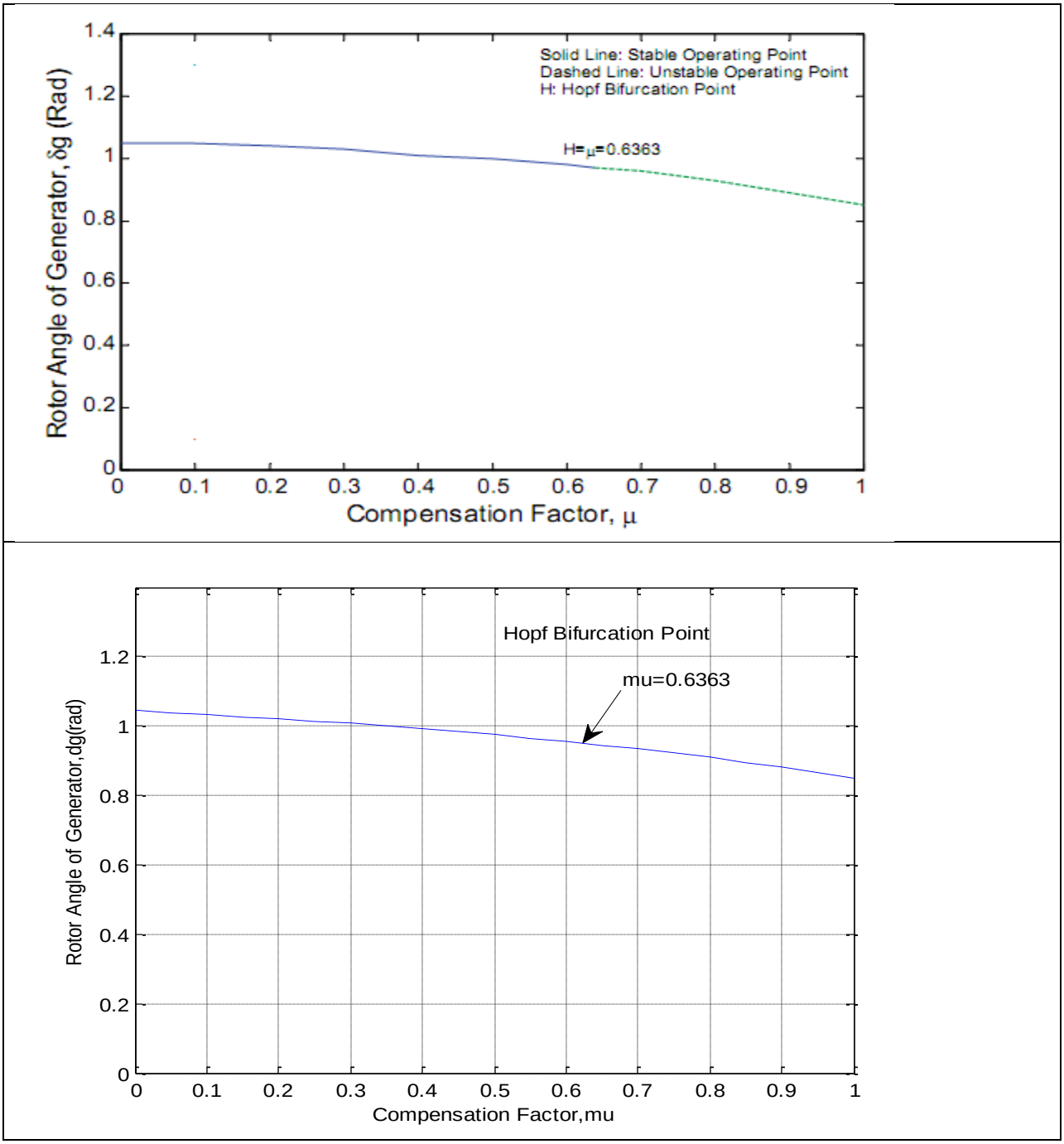

Fig8. Bifurcation diagram with k_R=1000, rotor angle of generator δ_g as a function of the compensation factor μ; the first one is of this paper and the second one is of mine.

The study of the operating point bifurcation is repeated for an AVR gain k_R=2000.Now, the Hopf bifurcation took place at a compensation factor μ=H≈0.5296.The bifurcation diagram for this case is shown in fig9.The system has a stable operating point in the range 0<μ<0.5296, unstable operating point in the range 0.5296<μ<1 and a Hopf bifurcation point at μ=H≈0.5296.

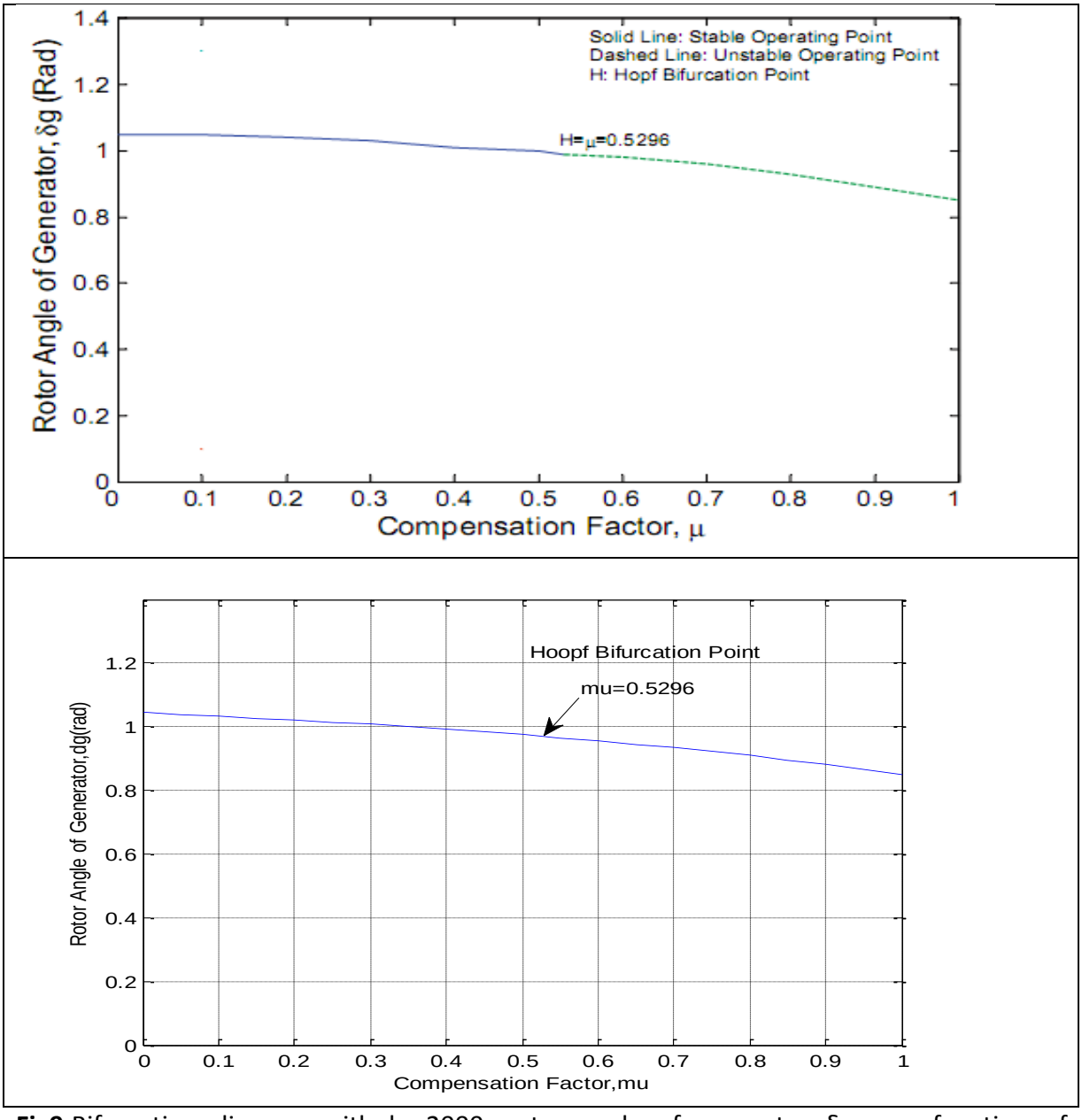

Fig9. Bifurcation diagram with k_R=2000, rotor angle of generator δ_g as a function of the compensation factor μ; the first one is of this paper and the second one is of mine.

So far we find out that the AVR gain affects the location of the Hopf bifurcation point of the system. The variation of the Hopf bifurcation point as a function of AVR gain is shown in fig.10 for two operating point with (pe=0.9 pu ; Qe=0.43 pu) and (pe=o.5 pu ; Qe=0.2 pu).in the first condition As the AVR increases, the Hopf bifurcation point increases up to a gain of about 1000.in the second condition this value is about 900.Therefore,for this system An AVR gain in the range of 1000 is the best from the operating point stability region point of view.

Time domain simulations for system have been carried out based on the nonlinear dynamical mathematical model with different compensation levels and AVR gains. The response of the system after a 0.02 pu step decrease on the infinite bus voltage applied at t=10s are shown in figs 11,12,13,14,15,16.

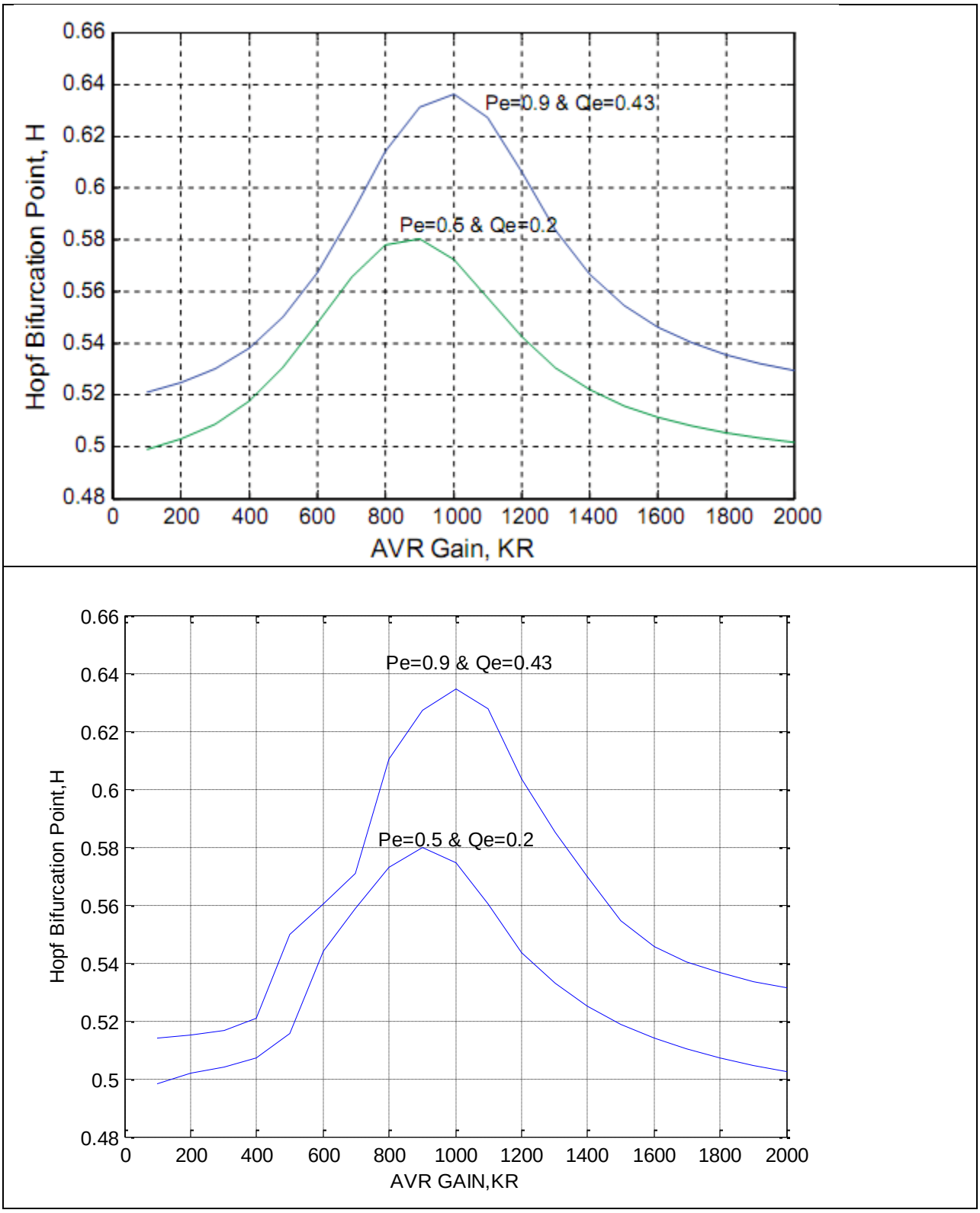

Fig10. Hopf bifurcation points as function of AVR gain k_R for two operating points; the first one is of this paper and the second one is of mine.

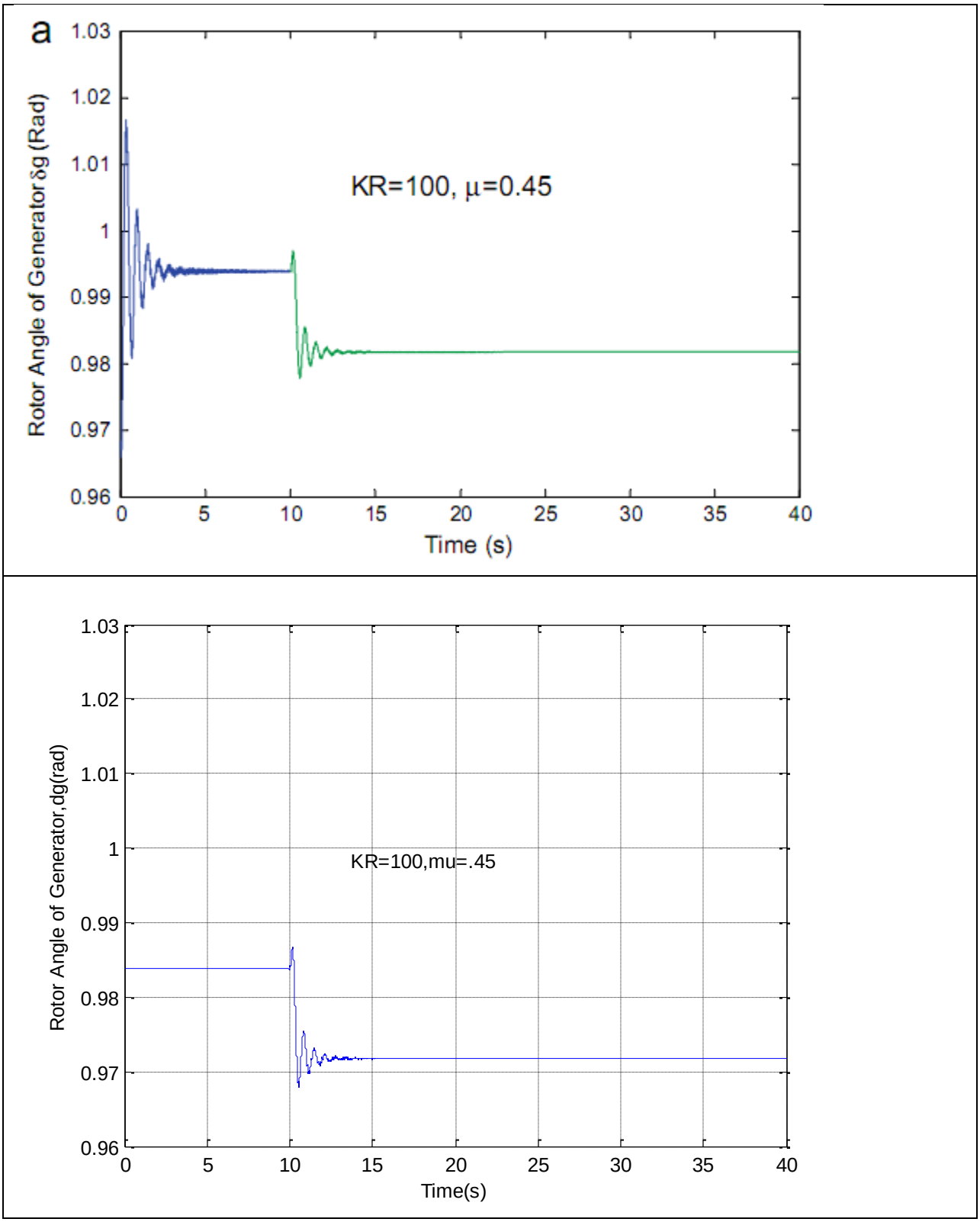

Fig11. Rotor angle of generator δ_g response at μ=0.45 after a 0.02 pu step decrease in the infinite bus voltage with k_R=100; the first one is of this paper and the second one is of mine.

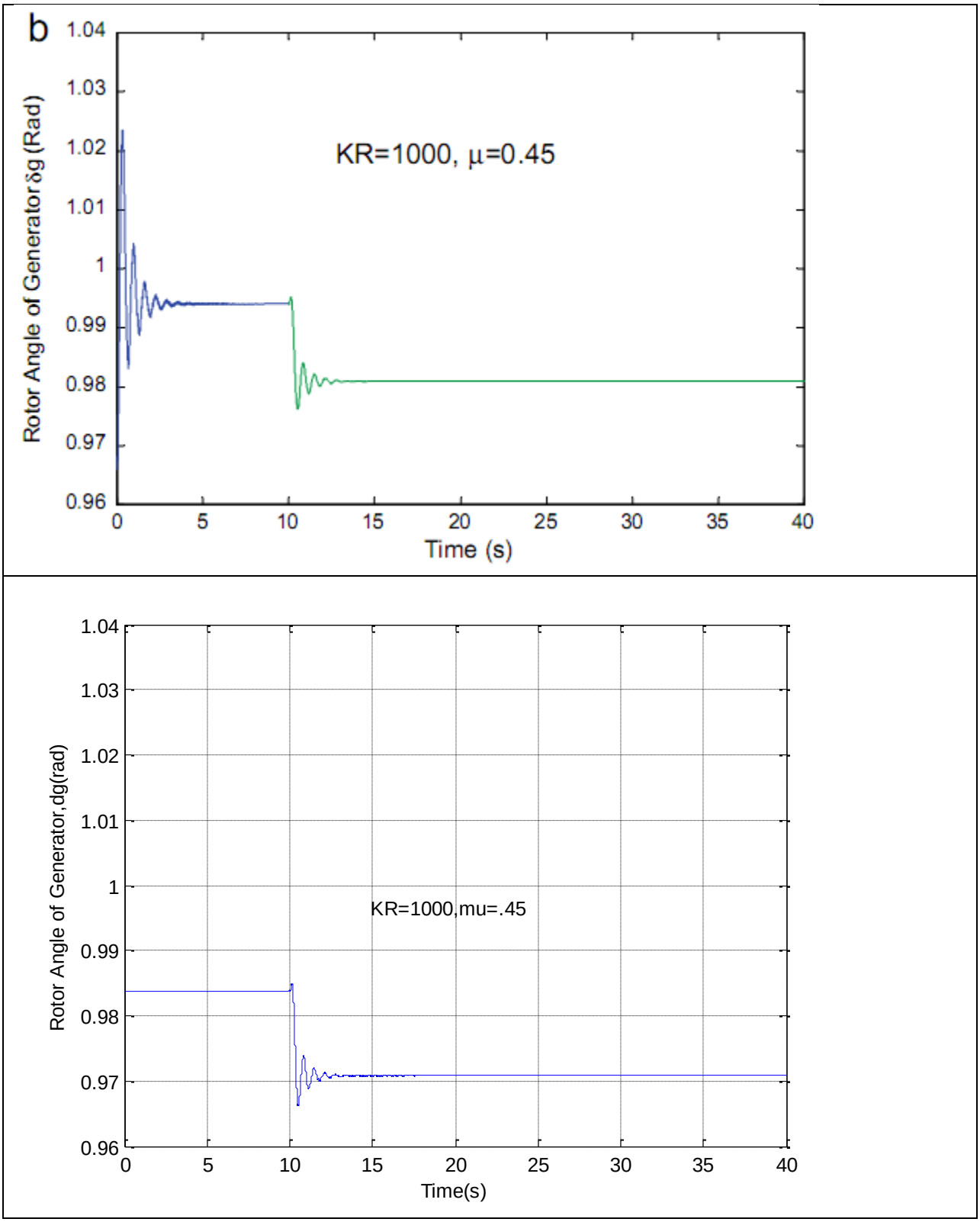

Fig12. Rotor angle of generator δ_g response at μ=0.45 after a 0.02 pu step decrease in the infinite bus voltage with k_R=1000; the first one is of this paper and the second one is of mine.

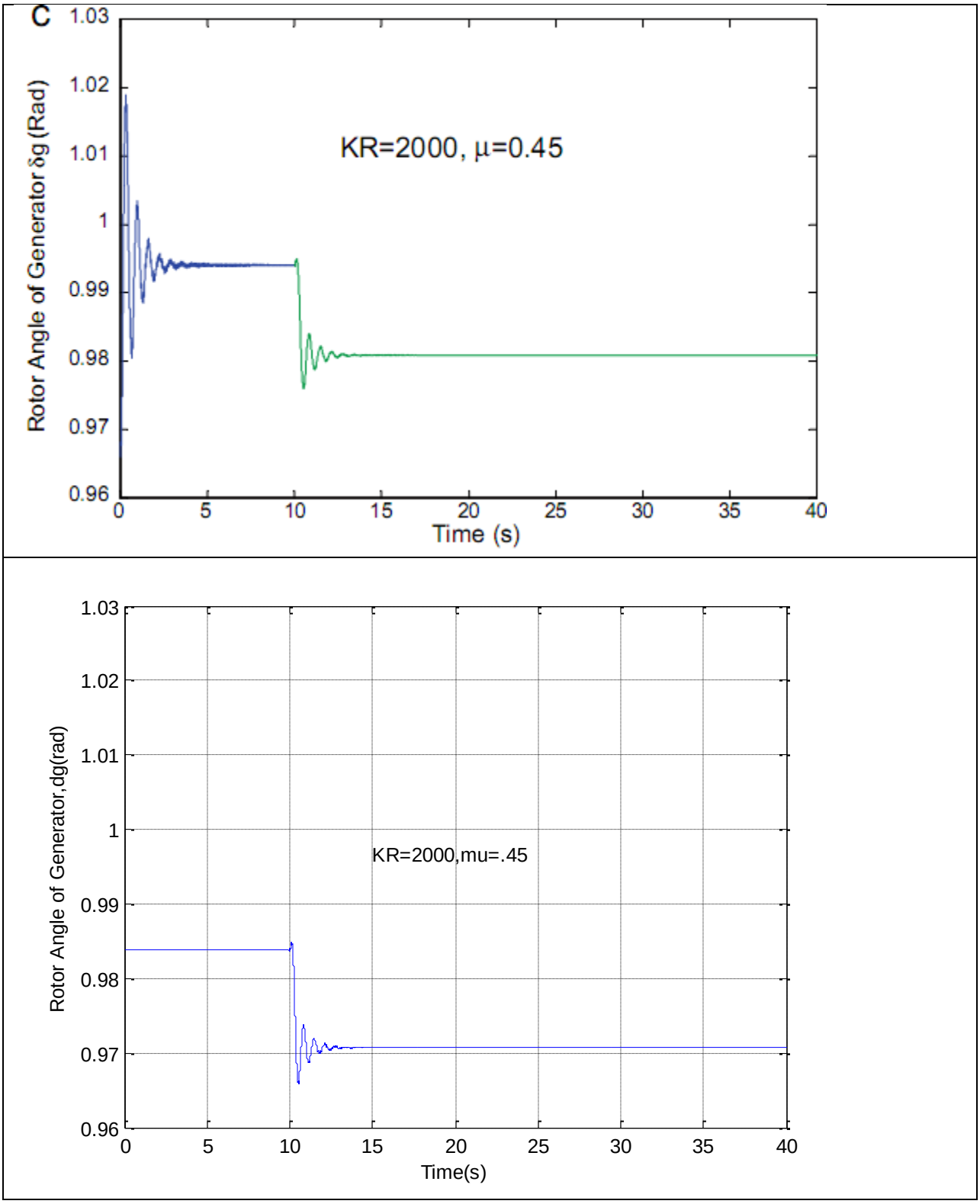

Fig13. Rotor angle of generator δ_g response at μ=0.45 after a 0.02 pu step decrease in the infinite bus voltage with k_R=2000; the first one is of this paper and the second one is of mine.

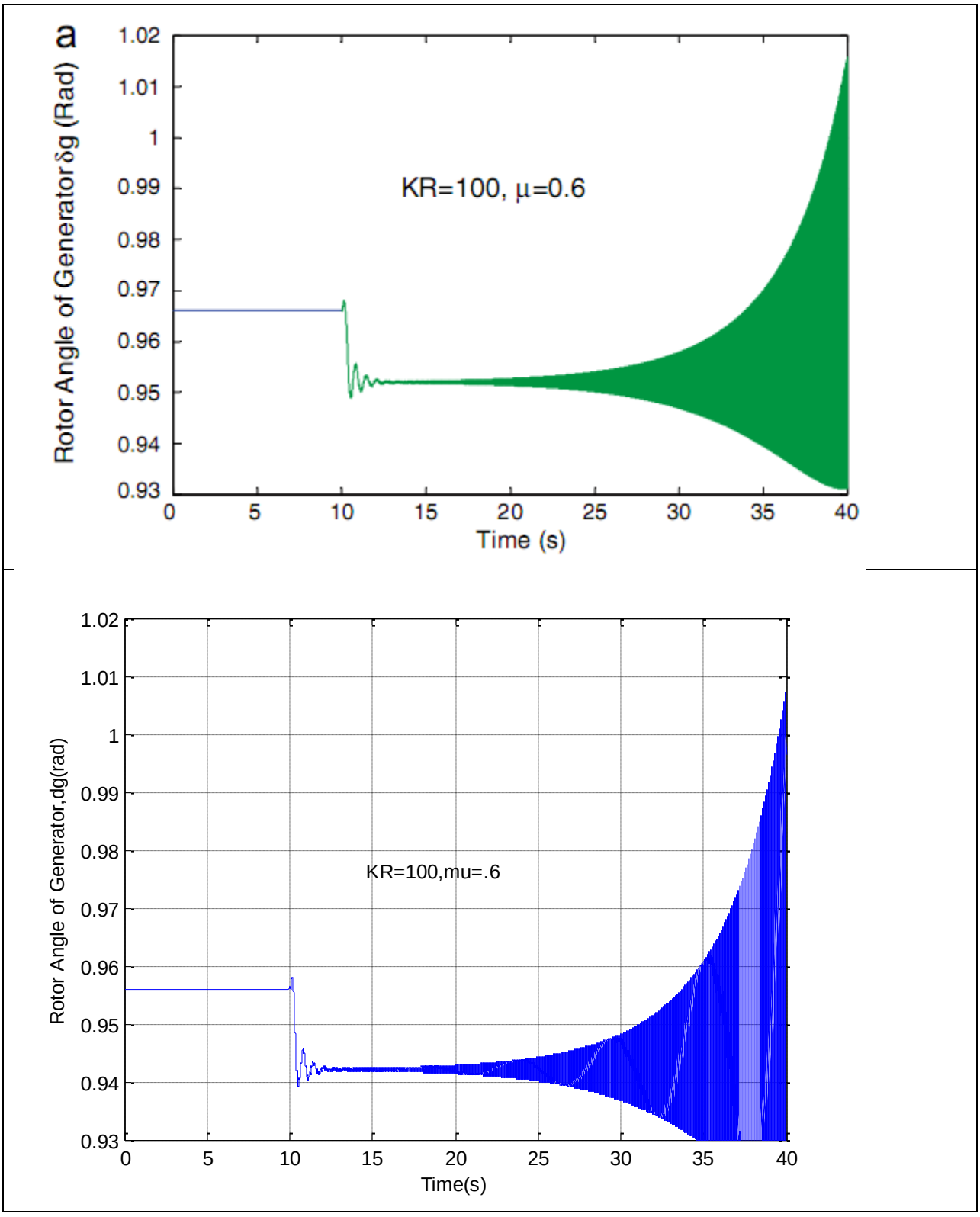

Fig14. Rotor angle of generator δ_g response at μ=0.6 after a 0.02 pu step decrease in the infinite bus voltage with k_R=100; the first one is of this paper and the second one is of mine.

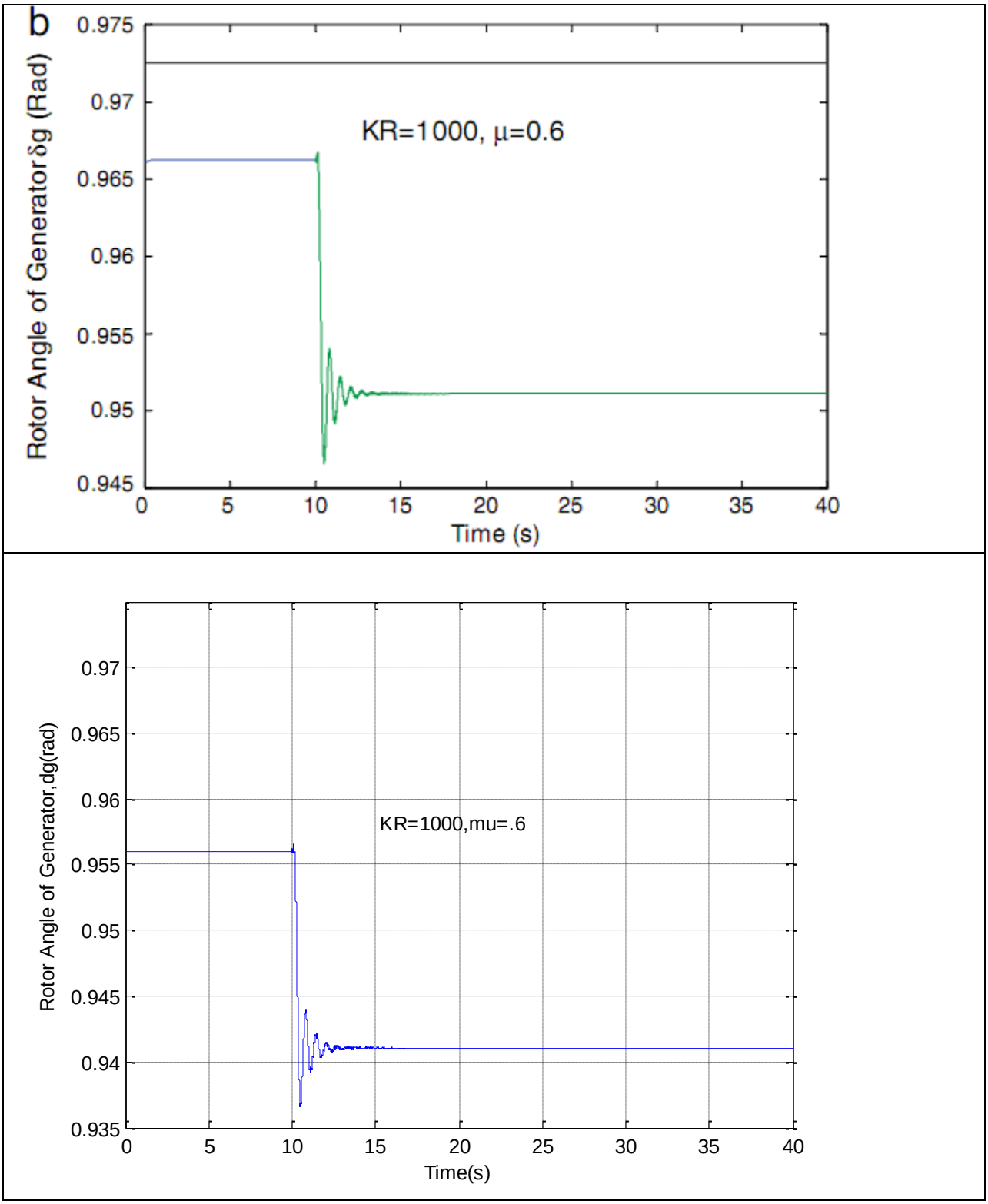

Fig15. Rotor angle of generator δ_g response at μ=0.6 after a 0.02 pu step decrease in the infinite bus voltage with k_R=1000; the first one is of this paper and the second one is of mine.

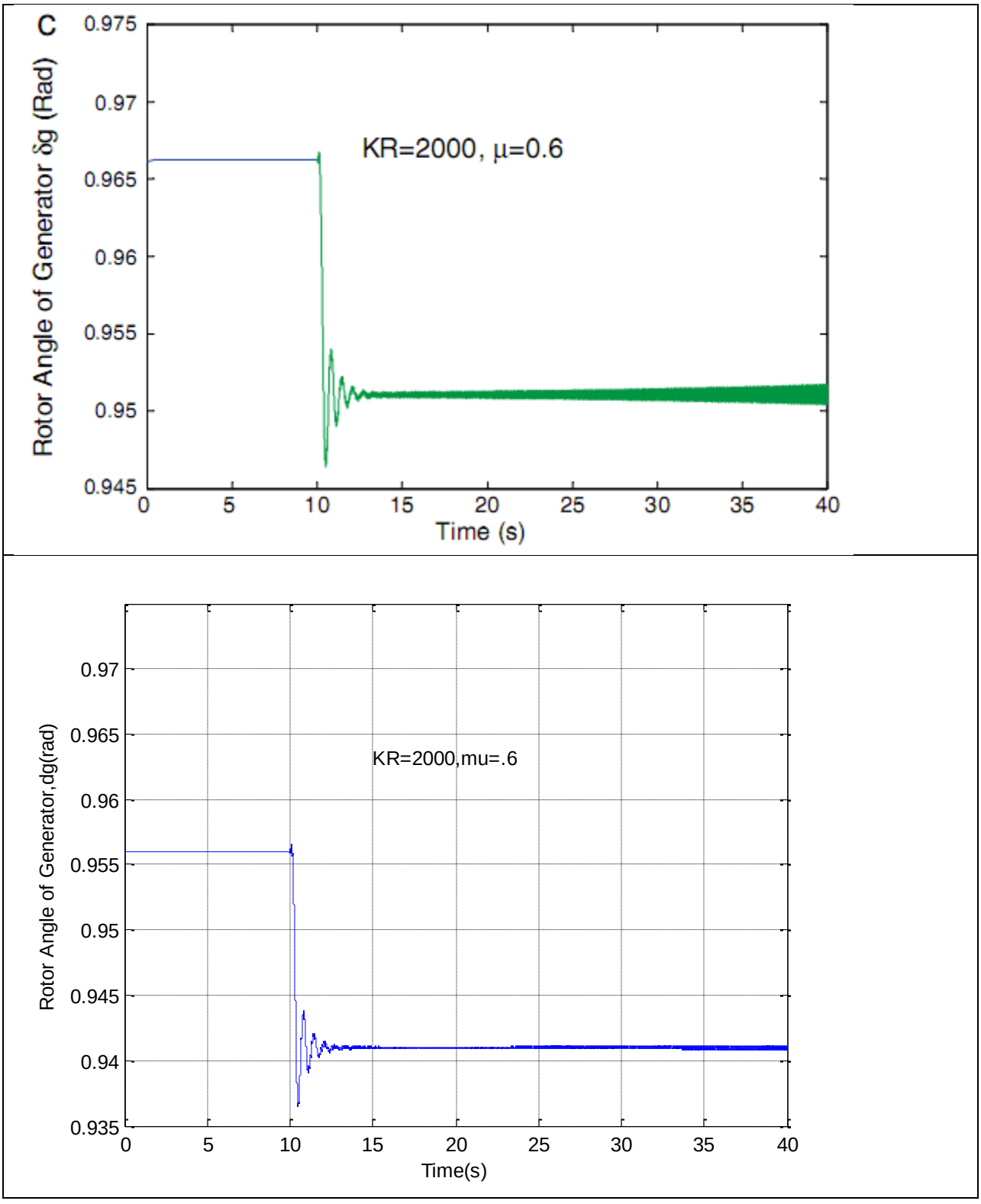

Fig16. Rotor angle of generator δ_g response at μ=0.6 after a 0.02 pu step decrease in the infinite bus voltage with k_R=2000; the first one is of this paper and the second one is of mine.

Conclusions

In this paper it is found that the AVR gain affects the location of the Hopf bifurcation point. For this system an AVR gain in the range of 1000 provides the best bifurcation point location. The time domain simulations coincide with the results of the bifurcation analysis.

Appendix

Synchronous generator (in pu on the base of generator ratings)

x_d=1.65;x_q=1.69;x_{akd}=1.51; x_{akq}=1.45; x_{kkd}=1.642; x_{kkq}=1.5238;
x_{ffd}=1.6286; x_{afd}=1.51; x_{fkd}=1.51;
r_a=0.0045;r_{fd}=0.00096;r_{kd}=0.016;r_{kq}=0.0116.

Mechanical system (in pu on the base of generator ratings)

M_1=0.0138;D_1=0.0014;k_{1g}=3.7363;M_g=1.7581;D_g=0.1758;k_{g2}=83.3823;

M_2=3.1004;D_2=0.3100;k_{23}=42.6572;M_3=0.4980;D_3=0.0498.

AVR and PSS

K_R=100-2000;T_R=0.025;T_w=10s;k_s=2;T_1=0.048s;T_2=0.032.